

**Detection and Monitoring of Cracks in a Concrete Buffer from DIC and AE
Measurements – 14439**

Lou Areias¹, Lincy Pyl², Sokratis Iliopoulos², Jun Gu², Dimitrios G. Aggelis², Bart Craeye³,
Geert De Schutter⁴, Robert Gens⁵, Philippe Van Marcke⁵, Erik Coppens⁵ and Alain Van
Cotthem⁶

¹EIG EURIDICE & VUB

²MeMC/VUB

³Betonadvies Gijko

⁴Magnel Laboratory for Concrete Research

⁵ONDRAF/NIRAS

⁶Tractebel Engineering SA

ABSTRACT

A second half-scale test has been performed in 2013 to obtain further insight into the feasibility to construct the Belgian Supercontainer (SC). This test incorporated new and innovative monitoring techniques to study the initiation and propagation of cracks in the buffer. They included Digital Image Correlation (DIC), Acoustic Emission (AE) and optical fibre sensors. The DIC and AE monitoring installations successfully identified the time of initiation of the first micro-cracks formed on the surface of the concrete buffer. The cracks measured approximately 15 ± 5 micrometres in width and formed less than one day after the start of the heating phase. AE results have been confirmed by DIC measurements, which both have been further confirmed by optical fibre as well as vibrating-wire strain measurements.

INTRODUCTION

ONDRAF/NIRAS, the Belgian Agency for Radioactive Waste and Enriched Fissile Materials, considers deep geological disposal in poorly indurated clay as the reference solution for the long-term management of high-level waste (HLW). The current concept for the packaging of HLW is the so-called Supercontainer (SC). The SC is a multi-barrier containment system mainly consisting of a hermetically sealed carbon steel overpack and a surrounding highly-alkaline concrete buffer. The SC is the Belgian reference concept for the packaging of HLW, which includes vitrified high-level radioactive waste and spent fuel [1, 2]. A conceptual view of the SC appears in Figure 1.

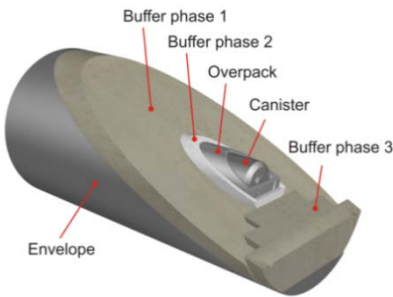


Fig. 1. Belgian Supercontainer concept.

The primary safety function of the buffer is to create high alkaline conditions around the carbon steel overpack in order to passivate the metal surface and ensure a very slow and uniform corrosion rate during the thermal phase. The thermal phase lasts several thousands of years. During this phase the carbon steel overpack will retain the radionuclides. In addition, the buffer provides radiological shielding during construction and transport of the SC. In a test performed in 2009 to evaluate the feasibility to construct the SC [3, 10], micro-cracks formed on the surface of the concrete buffer. The absence of a crack-monitoring system precluded defining the time of initiation, origin, evolution as well as the width and depth of penetration of these micro-cracks. A recent test performed in 2013 addressed these issues by including a monitoring system dedicated to the detection and evolution of cracks in the buffer. This system included the installation of DIC, AE and fibre optic sensors.

The monitoring installation successfully detected the onset of cracks in the concrete buffer. The analysis of the monitoring data is on-going to fully characterise these cracks. This includes determining the origin, size and extent of the cracks as well as evaluating their potential influence on the performance of the buffer. It will be possible to evaluate the impact of the cracks on the performance of the SC and to provide remedial measures, if needed, only after completion of the full analysis of the monitoring data.

APPLICATION OF DIC AND AE TO MONITOR CRACKS IN CONCRETE

DIC is a full field, non-contact, non-destructive optical technique that allows the identification of displacements between subsequent images taken by a pair of cameras [4, 5, 6], based on a black and white pattern fixed on the Area Of Interest (AOI) of the object under study. Figure 2 shows a typical setup of the DIC method.

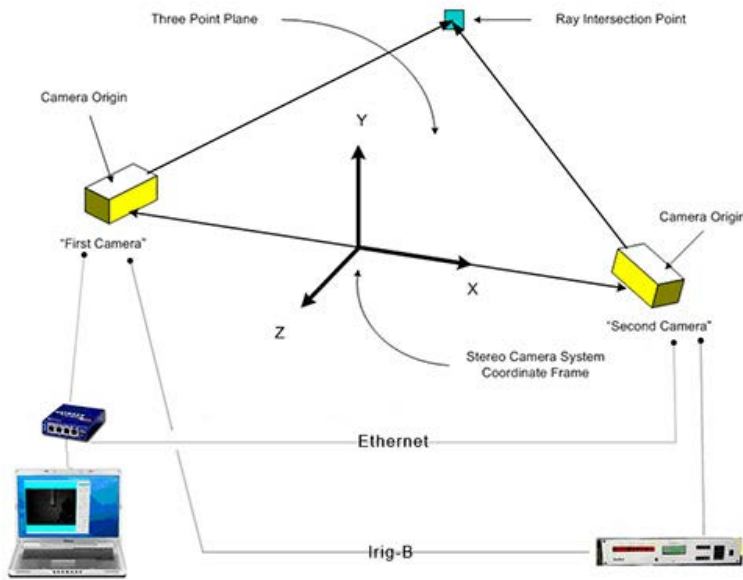


Fig. 2. Typical DIC setup.

The initial image processing involves defining a unique correlation area, known as the AOI, across the imaging area. The size of the AOI varies according to the surface one wants to monitor. Usually, the first image is taken in a non-deformed state while subsequent images are taken at different load stages. These facets are tracked in each successive image with sub-pixel accuracy. Sub-pixels are separately addressed elements of a pixel. To attain tracking with sub-pixel resolution, an image-based tracking algorithm is used. Then, using photogrammetric principles, the 3D coordinates of the entire surface of the specimen are precisely calculated. The results are the 3D shape of the component, the 3D displacements and the plane strain tensor.

Preliminary laboratory tests performed to evaluate the application of DIC to detect the initiation of cracking in concrete [7] showed that the DIC method can measure micro-cracks with a crack opening resolution of approximately 12.5 ± 5 micrometres. This is sufficiently sensitive to detect the formation of potential micro-cracks in the concrete buffer of the SC.

AE utilizes the transient elastic waves emitted by the tip of a crack during propagation. These waves are detected by piezoelectric sensors mounted on the surface of the concrete and are transformed into electric waveforms. AE provides information on the density of cracks, the geometric location and depth of the cracking sources (when installing sensors in the three dimensional space), while enabling the characterization of the mode of cracking [8]. A typical setup appears in Figure 3.

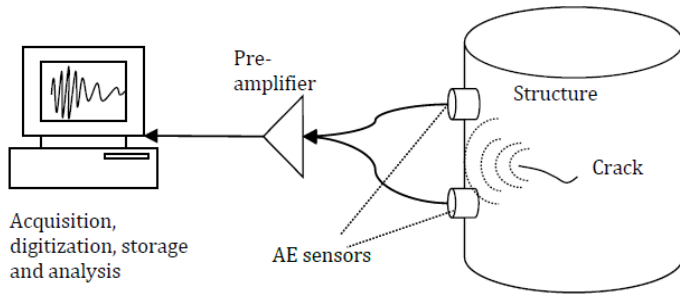


Fig. 3. Typical AE setup to monitor cracking in a concrete structure.

DESCRIPTION

An overview of the setup used for the second SC half-scale test (HST2) appears in Figure 4. The so-named half-scale test has a true diameter scale, while its height is limited to approximately half of that of a real SC [3, 10]. As seen in Figure 4, the HST2 integrates two separate moulds: an outer mould for the construction of the concrete buffer; and an inner mould to create the opening necessary for the installation of the heated overpack. Both moulds use a re-usable steel construction to reduce costs when repeating the test.

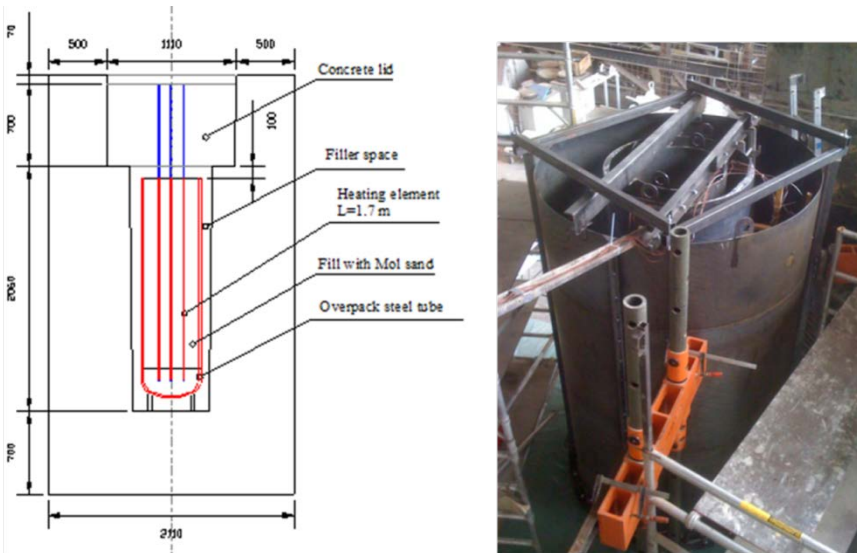


Fig. 4. Cross-sectional view of the HST2 [left] and test setup showing the outer and inner metal moulds [right].

Generally, the DIC's black and white digital image pattern is printed on a plastic film and then glued onto the surface of the AOI of the object. This requires a dry surface for proper adherence of the glue. In the case of the HST2 experiment, it was important to start

measurements as soon as possible after casting in order not to miss the first development of cracks. However, the presence of moisture on the concrete surface during the first days following casting did not permit the gluing of a plastic film on the concrete surface. In fact, the plastic film would run the risk of peeling off as a result of pressure and temperature build up on the concrete surface due to the hydration process. To solve this problem, a technique was developed, whereby the digital pattern was projected directly onto the concrete surface without the need to glue it [7]. Doing so enabled the installation of the digital image just two days after casting.

As shown in Figure 5, the outer steel mould contains three windows. The windows are removable to provide access for the installation of the DIC black and white speckle patterns as well as to take measurements during the test. The speckle pattern drawn in window 2, two days after casting, and the four AE sensors installed at each corner of the window are shown in the same figure. The AE sensors were installed on the steel mould during the first 28 days of curing and then attached directly to the concrete surface when the mould was removed.

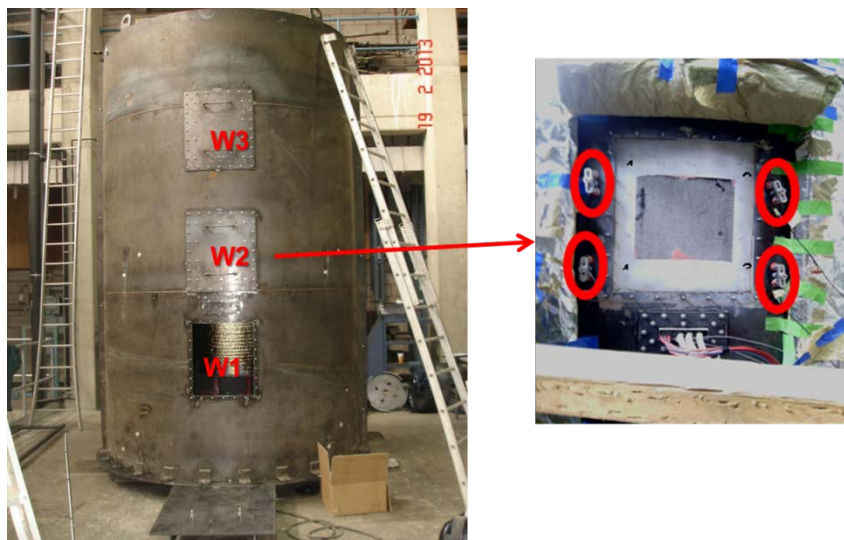


Fig. 5. Outer mould showing the three removable access windows for the DIC measurements [left] and printed speckle pattern together with four AE receivers installed in window nr. 2 [right]

RESULTS

The DIC and AE measurements did not show any evidence of cracks during the first phase of the test. The first phase represents the first 56 days of testing, before the installation of the heated overpack. During this phase, the monitoring installation measured only dilation and shrinkage of the buffer generated by the hydration and

hardening of the concrete. These results are in line with model predictions [9], which suggest a low probability of developing cracks during the first phase of the test. They also agree with both visual observations as well as physical measurements of strain obtained from Fibre Bragg Grating (FBG) optical fibres and vibrating wire (VW) sensors installed in the concrete buffer. In addition, the results also confirm observations made during the first half-scale performed in 2009 [3], where no cracks developed in the concrete buffer during the first phase of the test.

In the first phase of the test, during the first two days following the casting of the buffer on 16th of April, 2013, AE measurements registered a high number of hits, as shown in Figure 6. The measured AE activity is mostly due to the initial settlement of the concrete and the effects of hydration.

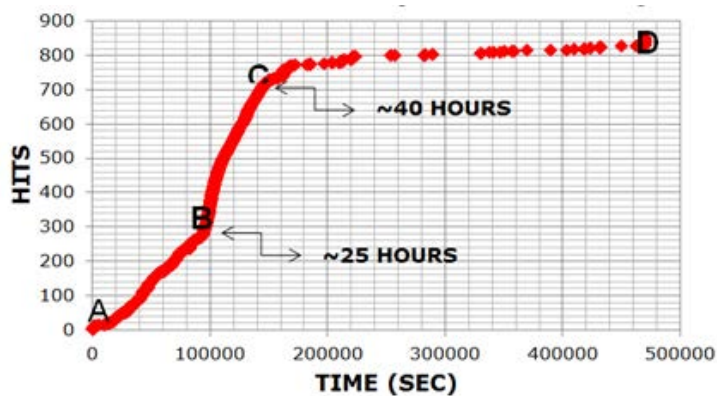


Fig. 6. Measurements in the beginning of the first phase of the test showing cumulative AE hits recorded in Window 2.

The heated overpack was installed in the buffer on the 10th of June, 2013. The day after, the concrete filler was cast to fill the void space left after the installation of the heated overpack. This marked the start of the second phase of the test. This phase lasted approximately 77 days. During this phase, the AE measurements successfully detected the onset of cracking in the buffer, as further described below.

The first cracks detected by the AE and DIC installations appeared in Window 2, just one day after the start of the heating phase. The initiation of the first cracks was marked by the sharp increase in AE hits shown in Figure 7 and confirmed by the visible image of the cracks given in Figure 8.

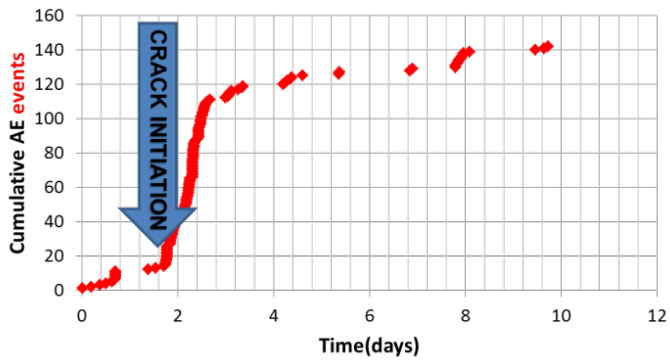


Fig. 7. Cumulative AE hits recorded in Window 2 during the first days following the start of the heated phase.

Figure 8 shows a digital image of Window 2 taken just prior to the start of the heating phase, showing the absence of cracks; and the same image taken the day after containing visible cracks. As mentioned, this image coincides with the sharp increase in recorded AE hits shown in Figure 7. Besides the detection of cracks in Window 2, other cracks appeared also in Windows 1 and 3 a few days later, as shown in Figure 9.

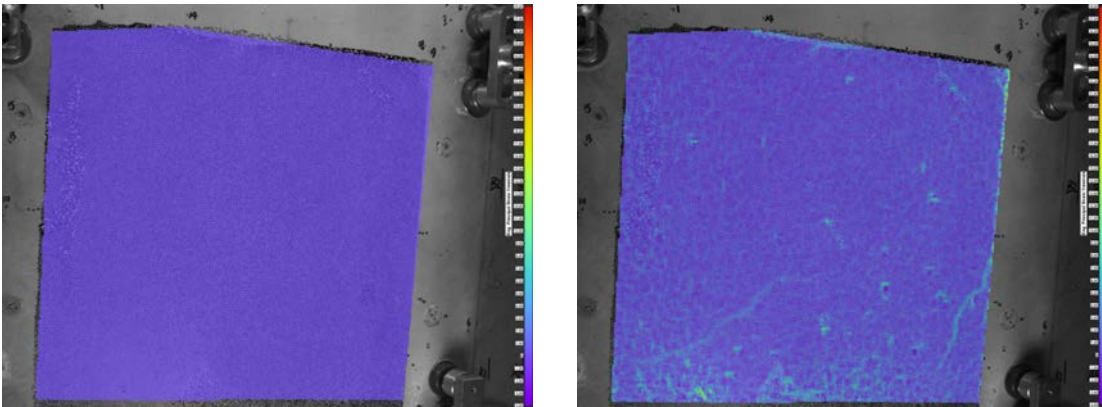


Fig. 8. DIC image taken at Window 2 just prior to the start of the heating phase [left] without cracks; and the same image taken a day after the start of the heating phase showing the presence of micro cracks [right].

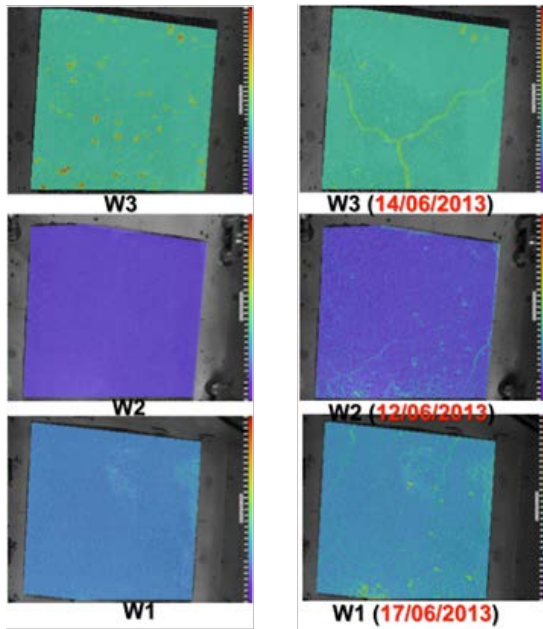


Fig. 9. [Left] DIC images of the three windows taken just prior to the start of the heating phase showing no cracks; and [right] same images taken at time of initiation of cracks, after the start of the heating phase.

The measurements of axial strain obtained from both FBG optical fibres and VW sensors installed in the concrete buffer provide additional confirmation of the DIC and AE measurements. These results appear in Figures 10 and 11, respectively.

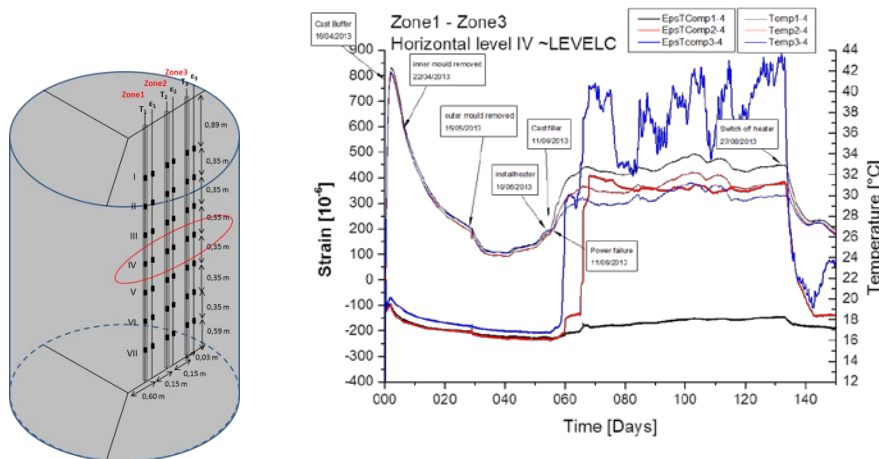


Fig. 10. Measurements of axial strain [lower curves] and temperature from three FBG sensors installed at the mid-level of the HST2.

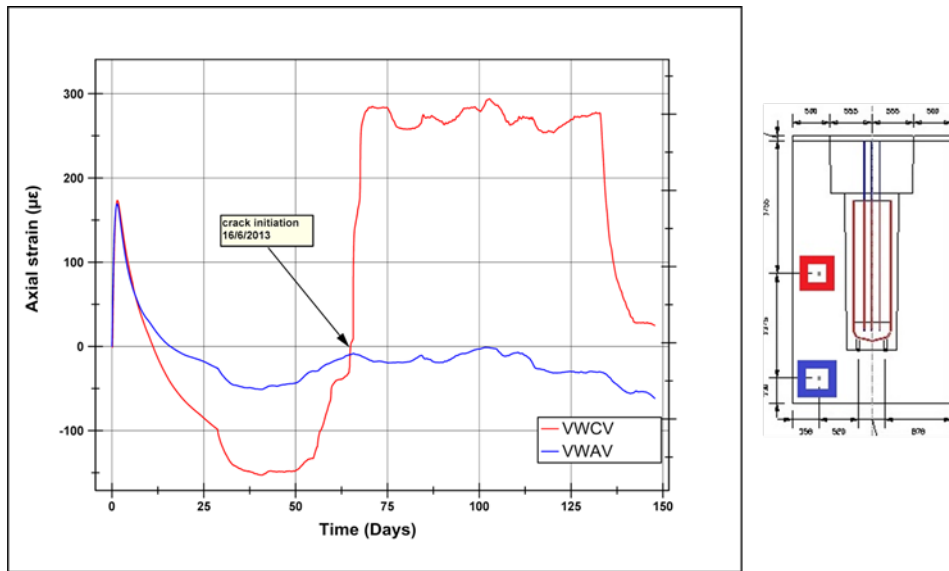


Fig. 11. Measurements of axial strain from two VW sensors installed at the mid and lower levels of the HST2.

The results shown in Figure 10 give the temperature as well as the axial strain profiles obtained by three FBG optical sensors installed at the mid height of the buffer. The sensors are located at three different radial distances in the concrete structure, as shown. The sharp increase in strain measured at the sensor in Zone 2, located approximately in the middle of the concrete buffer wall, and the one in Zone 3, close to the outer wall of the buffer, represent a crack at the level of Window 2.

Finally, the results in Figure 11, showing the measurements of axial strain from VW sensors located at the mid and low levels of the buffer, provide additional confirmation of the observations just presented. In particular, the VW sensor located in the middle of the buffer, which corresponds approximately to the location of the FBG sensor in Zone 2 in Figure 10, confirms the presence of a fracture and provides a good match of the strain profile measured by the same FBG sensor.

CONCLUSIONS

The DIC and AE techniques deployed in the second half-scale test to monitor the initiation and evolution of cracks on the surface of the concrete buffer confirmed the absence of cracking during the first phase of the test, before the installation of the heated overpack, confirming both model results as well as visual observations made during the test.

The installation successfully detected the first cracks that appeared in the buffer, which formed in Window 2 just one day after the start of the heating phase. Later on, the installation was also able to detect the initiation of other cracks observed at the other two

windows. These results have been confirmed by strain measurements obtained from VW and FBG optical sensors as well as by visual observations.

The analysis of the monitoring data, which includes the origin, size and extent of the cracks, is on-going to fully characterise these cracks. These results will contribute to a further study to evaluate the impact of these cracks on the performance of the SC.

REFERENCES

- [1] ONDRAF/NIRAS (2009), "The Long-Term Safety Strategy for the Geological Disposal of Radioactive Waste," ONDRAF/NIRAS report NIROND-TR 2009-14 E.
- [2] ONDRAF/NIRAS (2010), Feasibility strategy and Feasibility Assessment Methodology for the geological disposal of radioactive waste, report NIROND-TR 2010-19 E.
- [3] Areias, L., Craeye, B., De Schutter, G., Van Humbeeck, H., Wacquier, W., Villers, L., Van Cotthem, A. (2010). Half-scale test: an important step to demonstrate the feasibility of the Belgian Supercontainer concept for disposal of HLW. Proceedings 13th International Conference on Environmental Remediation and Radioactive Waste Management, ICEM2010, Tsukuba, Japan.
- [4] Vasilakos, I., Belkassam, B., Sol, H., Verbert, J., Duflou, J. (2009), "Study of deformation phenomena in Single Point Incremental Forming by means of Digital Image Correlation technique", Optical Measurement Techniques for Structures and Systems, pp. 379-388
- [5] Sutton MA, Ortu JJ, Schreier HW (2009). Image correlation for shape, motion and deformation measurements. Basic concepts, theory and applications. New York, USA: Springer Science + Business Media.
- [6] Słominski C., Niedostatkiewicz M., Tejchman J. (2006). Deformation measurements in granular bodies using a Particle Image Velocimetry technique, *Archives of Hydro-Engineering and Environmental Mechanics*, **53** (1), 71–94.
- [7] Areias, L., H. Sol, G. Jun, L. Pyl, Ph. Van Marcke, E. Coppens, J. Verstricht, L. Villers and A. Van Cotthem (2013). The application of DIC to detect potential onset of micro-cracking in the concrete buffer of the Supercontainer, Monitoring in Geological Disposal of Radioactive Waste, MoDeRn Conference and Workshop, Luxembourg, 19-21 March 2013.
- [8] Aggelis, D. G., S. Verbruggen, E. Tsangouri, T. Tysmans, D. Van Hemelrijck (2013). Characterization of mechanical performance of concrete beams with external reinforcement by acoustic emission and digital image correlation, *Construction and Building Materials* 47 (2013) 1037–1045.
- [9] Craeye, Bart (2010) Early-Age Thermo-Mechanical Behaviour of Concrete Supercontainers for Radwaste Disposal, PhD thesis, University of Ghent.
- [10] Areias, L., I. Troullinou, S. Iliopoulos, E. Voet, L. Pyl, Ch. Lefevre, J. Verstricht, Y. Van Ingelgem, E. Coppens and Ph. Van Marcke (2013). Instrumentation and monitoring aspects of a ½-scale test to evaluate the feasibility of the Belgian

WM2014 Conference, March 2 – 6, 2014, Phoenix, Arizona, USA

Supercontainer, 15th ASME International Conference on Environmental Remediation and Radioactive Waste Management.